



Assessment of Dynamic Response of Cohesionless Soil Using Strain-Controlled and Stress-Controlled Cyclic Triaxial Tests

Shiv Shankar Kumar · A. Murali Krishna · Arindam Dey

Received: 30 April 2018 / Accepted: 15 October 2019 / Published online: 2 November 2019
© Springer Nature Switzerland AG 2019

Abstract Soils subjected to earthquake motions undergo random variations in stress, strain and frequency during the entire period of shaking. The spatial and temporal complexity of the strong motions is commonly addressed through simplistic strain-controlled or stress-controlled cyclic loading tests as a part of laboratory investigations. Such a methodology is utilized and reported in the present study for assessing the dynamic response of cohesionless sand obtained from River Brahmaputra, India. In order to assess the dynamic response and liquefaction potential of the cohesionless Brahmaputra sand, both stress-controlled and strain-controlled cyclic triaxial tests were performed on reconstituted cylindrical specimens prepared at different relative densities (D_r)

ranging from 30 to 90%. The specimens were subjected to varying effective confining pressures (σ'_c : 50–200 kPa), shear strain amplitudes (γ : 0.015–4.5%) and cyclic stress ratios (CSR: 0.05–0.3). For all the tests, the frequency of the applied harmonic loading was maintained at 1 Hz. The magnitude of excess pore-water pressure (PWP) generated during successive loading cycles of the strain-controlled tests was found to be considerably lower than that generated in a stress-controlled test. The strain-controlled test reveals a reduction in the development of excess PWP with the increase in confining pressure and relative density, thereby indicating a decrease in liquefaction potential with increasing confining pressure. The stress-controlled test highlighted that based on a particular CSR, an increase in confining pressure results in the requirement of higher deviatoric stress and smaller numbers of cycles are required to initiate liquefaction. Although apparently misleading, it is imperative that during earthquake, same deviatoric stress is applied on the entire soil deposit. Thus, for specimens at larger depths having higher confining pressure, the CSR value is smaller, and thereby successive deeper layers require more number of stress cycles to liquefy. Hence, the study revealed that both stress-controlled and strain-controlled tests can be successfully used to assess the dynamic properties and liquefaction potential of cohesionless specimens. Based on the findings, the developed cyclic shear stress ratio (CSR) = 0.5 and cyclic shear strain amplitude (γ) = 0.5% are

S. S. Kumar (✉)
School of Civil Engineering, Kalinga Institute of
Industrial Technology Bhubaneswar, Bhubaneswar,
Odisha 751024, India
e-mail: shivshankar.mit@gmail.com;
k.shiv@iitg.ernet.in

A. Murali Krishna
Department of Civil and Environmental Engineering,
Indian Institute of Technology Tirupati, Tirupati,
Andhra Pradesh 517506, India
e-mail: amk@iittp.ac.in

A. Dey
Department of Civil Engineering, Indian Institute of
Technology Guwahati, Guwahati, Assam 781039, India
e-mail: arindamdeyitg16@gmail.com

considered as the limiting conditions to achieve the onset of liquefaction through strain-controlled and stress-controlled approaches, respectively.

Keywords Strain-controlled · Stress-controlled · Cyclic triaxial test · Cyclic stress ratio · Pore water pressure · Dynamic soil properties

1 Introduction

Soil mass encountered with earthquake motions reflects varying amplitude of stresses and strains throughout the duration of shaking. For the better comprehension of the design of earthquake resistant structures, it is necessarily important to assess the dynamic characteristics of soil subjected to the realistic strong motions. Due to inherent irregularity and complexity of the earthquake motions and their associated properties, the accurate estimation of dynamic properties and responses of soils are challenging task. Several researchers have conducted strain-controlled and stress-controlled laboratory investigations employing regular harmonic excitations for the dynamic characterization of soils (Seed and Lee 1966; Dobry et al. 1982; Ishihara 1993; Lombardi et al. 2014; Chattaraj and Sengupta 2016). The regular harmonic excitations are derived from irregular seismic excitations based on an energy equivalency with the actual strong motion, thereby obtaining the adaptable number of constant-amplitude strain or stress cycles to be used in the laboratory tests (Ishihara and Yasuda 1972). It has been reported that when saturated soil deposits subjected to regular harmonic loading, either by strain- or stress-controlled manner, the generated variations in the excess pore-water pressure (PWP) are primarily responsible to alter the strength characteristics of the soil (Matasovic and Vucetic 1992). Seed and Idriss (1970) and Dobry et al. (1982) were the pioneering researchers to introduce the cyclic stress- and strain-controlled approach, respectively, to qualify the liquefaction resistance of soils with the variations in excess PWP. As the name suggests, cyclic stress approach considers the generation of excess PWP and resulting strains to be primarily governed by the seismic loading expressed in terms of the constant amplitude cyclic shear stresses; while, in cyclic strain approach, the

constant-amplitude cyclic shear strains control the generation of excess PWP and associated shear stresses (Kramer 1996). It has been stated that, practically, the conversion of an irregular acceleration-time history to a cyclic stress history is comparatively easier than converting the former to a cyclic strain history (Kramer 1996). Earthquake motions being irregular and random where both the cyclic shear stresses and cyclic shear strains vary simultaneously, it is important to characterize the dynamic response of the soil based on both strain-controlled and stress-controlled tests to reach at a comprehensive understanding of its field behavior. In order to represent the complex strong motions (that vary in amplitude and frequency during the entire duration of the motion), both strain-controlled and stress-controlled tests are used for simplistically addressing the dynamic response of the specimen. Strain controlled cyclic tests are used to determine the strain-dependent dynamic properties of the specimen, namely the shear modulus, shear modulus degradation curve, and the damping ratio. On the other hand, the stress-controlled cyclic tests are generally used to assess the liquefaction related parameters of the specimen subjected to cyclic loads, namely the number of cycles and the cyclic stress ratio (CSR) required for the onset of liquefaction in a cohesionless specimen. However, since both the tests involve the measurement of excess pore-water pressure developed during the cyclic tests, both stress-controlled and strain-controlled cyclic triaxial tests have been used in the present study for assessing the onset of liquefaction and other liquefaction related parameters of Brahmaputra sand.

A major portion of the Guwahati city thrives on the alluvial basin of River Brahmaputra. The water table in the region being near the surface for a major share of the annual duration, the alluvial beds mostly remains saturated. Moreover, Brahmaputra river bed sand, being available in plenty, is frequently used as a filling and construction material at most of the major construction sites in and around the Guwahati city. The region is located in the Seismic Zone V, one of the most seismically active locations of the country, and is often subjected to earthquakes of various magnitudes. The presence of the saturated sandy deposits makes the region susceptible to liquefaction. Substantial liquefaction, approximately over an area of 126 acres, was reported in the Guwahati city during the M8.6 1950 Assam-Tibet earthquake (Poddar 1950;

Raghukanth 2008). In this regard, it is extremely important to have a comprehensive dynamic characterization of BS based on both strain-controlled and stress-controlled tests, and the same has been reported in this article.

The present study investigates the dynamic response and liquefaction behavior of Brahmaputra Sand (BS) using both strain-controlled and stress-controlled cyclic triaxial tests, thereby highlighting the development of excess pore pressure leading to the strength loss of the specimen at different testing conditions. BS soil, used in this study, was collected from the bed of River Brahmaputra nearby the Guwahati City, Assam, India. The triaxial specimens were prepared at different relative densities, ranging from 30 to 90%. Cyclic triaxial tests were conducted at different effective confining pressure (σ'_c), shear strain amplitudes (γ) and cyclic stress ratio (CSR) values ranging 50–200 kPa, 0.015–4.5% and 0.05–0.3, respectively. For all the tests, the applied loading frequency of sinusoidal excitation was chosen 1 Hz.

2 Existing Literature

Several pioneer literatures are available on the evaluation of dynamic properties and liquefaction behavior of soils using strain-controlled and stress-controlled approach (Seed and Lee 1966; Lee and Seed 1967; Seed 1968; Seed and Idriss 1970; Seed and Peacock 1971; Castro 1975; Peck 1979; Dobry et al. 1982; Vucetic and Dobry 1988; Ladd et al. 1989; Ishihara 1993; Youd et al. 2001). It was reported that the increase of excess PWP in saturated sand deposits, during earthquake/cyclic loading, results in the reduction in internal friction and consequent loss of strength, thereby leading to liquefaction. Recently, Kumar et al. (2018a) and Dammala et al. (2019) have reported the importance of site-specific strain-dependent dynamic soil properties and soil liquefaction based on the ground response analysis, respectively. Kumar et al. (2018b) was utilized the stress-controlled irregular excitations to evaluate the soil response under different magnitude ground acceleration. Although the literatures are available, the comparable studies on the soil response utilizing both strain- and stress-controlled approach are scanty. Govindaraju (2005) had carried out both strain- and stress-controlled cyclic triaxial tests on cohesionless soils, and

reported that the generation of excess PWP during cyclic loading is potent to cause substantial damage to various geotechnical structures owing to the phenomenon of liquefaction. Lombardi et al. (2014) and Chattaraj and Sengupta (2016), have evaluated the liquefaction potential of sands using stress-controlled approach for its application in the analysis of soil-structure interaction. Apart from the amplitude and duration of earthquake induced cyclic loading, the generation of excess PWP required to initiate the liquefaction depends on the number of cycles, type of tests and soil type (Seed and Idriss 1970). It was also reported that in strain-controlled cyclic tests, the PWP build-up is negligibly affected by the specimen fabric and sample disturbance, while marginally affected by relative density (Dobry et al. 1982; Vucetic and Dobry 1988; Ladd et al. 1989). Apart from the utilization of cyclic triaxial test apparatus, strain-controlled and stress-controlled cyclic shear tests have also been conducted on sand-silt mixture specimens to evaluate their liquefaction potential using torsional shear test apparatus employing hollow specimens (Movahed et al. 2011). Sitharam et al. (2012) illustrated that the progressive degradation of stiffness and accumulation of strain during strain-controlled and stress-controlled tests, respectively, leads to the onset of liquefaction due to an increase in the excess PWP resulting in the softening of the soil specimen.

3 Material Used

Figure 1a presents the grain size distribution of BS soil, which shows that the chosen material is encompassed within the boundaries of severely liquefaction zone, as per the proposition of Tsuchida (Ishihara et al. 1980; Xenaki and Athanasopoulos 2003). Figure 1b depicts the Field Emission Scanning Electron Microscope (FESEM) image illustrating the sub-rounded shape of the grains of BS along with the meager presence of fine particles. Table 1 provides the index properties of the BS soil, as determined from laboratory tests as per the relevant Indian standard codal provisions. Based on the outcomes of the investigations, the test material is categorized as poorly graded sand (SP).

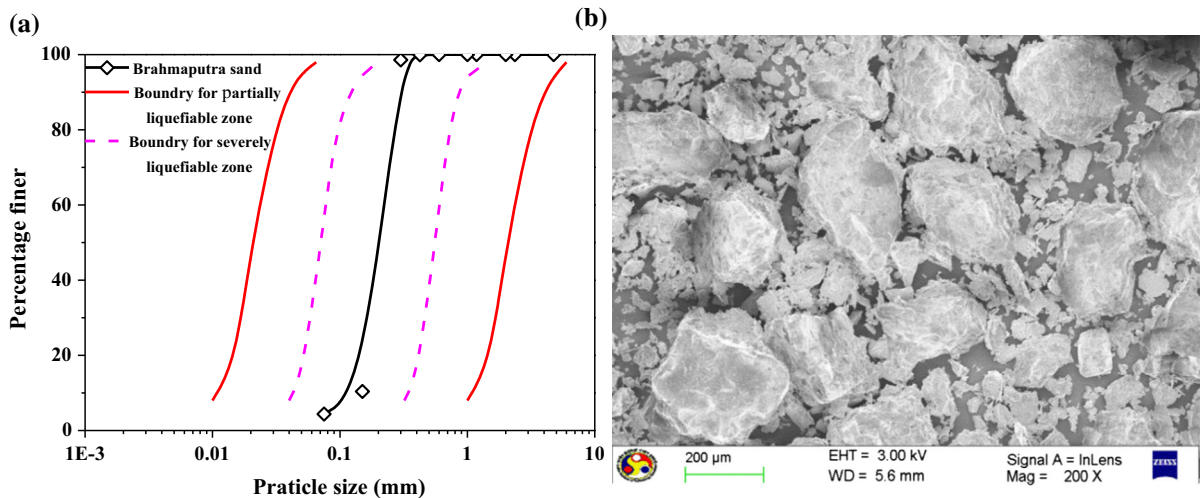


Fig. 1 a Particle size distribution, b FESEM image of BS

Table 1 Physical properties of sand

Soil descriptions	Values	Codal provision
Mean grain size, D_{50} (mm)	0.21	ASTM D6913
Minimum unit wt. (kN/m^3)	13.85	ASTM D4254
Maximum unit wt. (kN/m^3)	16.84	ASTM D4253
Uniformity coefficient (C_u)	1.47	
Coefficient of curvature (C_c)	1.09	
Specific gravity	2.7	ASTM D0854
Classification symbol	SP	ASTM D2487

4 Test Procedure and Programme

In the present study, an automated pneumatic controlled Cyclic Triaxial (CT) testing apparatus has been employed to conduct the experimental investigations. The details of the instrument and the adopted technique of sample preparation for cyclic shear tests are available in Kumar et al. (2017a, b). To evaluate the strain- and stress-dependent dynamic response of BS, a series of strain-controlled (ASTM D3999) and stress-controlled (ASTM D5311) undrained tests have been conducted. Since the primary objective of the reported work was to assess the dynamic parameters related to the liquefaction potential and liquefaction behaviour of the BS specimens, the stated four parameters (D_r , σ'_c , γ and CSR) are characteristically varied. D_r represents the relative density or the degree of compactness of cohesionless soil. σ'_c represents the

effective confining stress imparted on the specimen in field condition. γ represents the peak shear strain subjected to the soil specimen during its shaking under the motion of excitation. CSR is an index used to manifest the strength of soil under cyclic loading, which is described as the ratio of applied deviator stress to the effective confining stress (σ'_c) during a stress-controlled cyclic loading. Along with the above parameters, the numbers of cycles of loading is varied to assess the development and generation of excess pore-water pressure which is used to identify various states of liquefaction as described in the manuscript. All these parameters are well-established as indicators of soil liquefaction potential of soil (Kramer 1996), and hence the same are varied in the present study. Tables 2 and 3 present the investigating parameters as used in the experimentation scheme. Consideration of a specific value of frequency to perform the strain-controlled and stress-controlled cyclic tests is a challenging task, especially when the earthquake motion consists wide range of frequency. Based on the existing literatures on the effect of frequency on the dynamic behaviour of soils as well as on soil liquefaction, the frequency of 1 Hz was chosen for the applied harmonic regular excitations for all the tests reported in this study (Kramer 1996; Ishihara 1996; Teachavorasinskun et al. 2002; Yilmaz et al. 2004; Ravishankar et al. 2005; Bhattacharya 2007; Jakka et al. 2010; Maheshwari et al. 2012; Lombardi et al. 2014; Chattaraj and Sengupta 2017).

Table 2 Parameters of the strain-controlled cyclic triaxial tests

Soil	D_r (%)	σ'_c (kPa)	f (Hz)	γ (%)
BS	30	50	1	0.015, 0.045, 0.075, 0.15, 0.30, 0.45, 0.60, 0.75, 1.0, 1.5, 3.0
		100		0.045, 0.075, 0.15, 0.30, 0.45, 0.60, 0.75, 1.5
		150		0.045, 0.075, 0.15, 0.30, 0.45, 0.60, 0.75
	60	50		0.15, 0.60, 1.0, 1.5, 3.0, 4.5
		100		
		150		
	90	50		0.045, 0.075, 0.15, 0.30, 0.45, 0.60, 0.75, 1.5
		100		0.045, 0.075, 0.15, 0.30, 0.45, 0.60, 1.0, 1.5, 2.0
		150		0.045, 0.075, 0.15, 0.30, 0.45, 0.60, 0.75, 1.0, 1.5, 2.0

Table 3 Parameters of the stress-controlled cyclic triaxial tests

Soil	D_r (%)	σ'_c (kPa)	f (Hz)	CSR
BS	30, 60, 90	50, 100, 200	1	0.05, 0.1, 0.2, 0.3

5 Results and Discussions

5.1 Strain-Controlled Approach

Regular excitation is a simple and approximated way to find the behaviour of soils subjected to actual irregular excitations. This section discuss the results obtained from the strain-controlled cyclic triaxial tests (for 40 cycles at $f = 1$ Hz), in terms of excess PWP and cyclic stress ratio (CSR), at different γ , σ'_c and D_r . The variations in excess PWP is represented in terms of normalized PWP ratio, r_u ($= PWP/\sigma'_c$).

5.1.1 Variation of r_u at Different γ , σ'_c and D_r

Figure 2a shows the variations in r_u with number of cycles (N) at different γ for $D_r = 30\%$ and $\sigma'_c = 100$ kPa, indicating a nonlinear increase of excess PWP with number of cycles. For shear strain value of 0.3%, r_u value reached 1 (one) at about 12 cycles, indicating the attainment of liquefaction state. For shear strain values of 0.045% and 0.075%, the generated excess PWP ratios are within 0.6. The figure also shows that though the average (or maximum) r_u values increased with shear strain, the cyclic variations of r_u at any cycle decreased with the

increase in shear strain magnitude. The dotted lines present the maximum value of excess PWP, which has been further used in the analysis and corresponding interpretations. It can be observed that the possibility of the onset of soil liquefaction increases with the increase of γ and N . In other words, at any particular σ'_c , for identical N , the tendency of the specimen to liquefy increases with the increase in applied γ . Therefore, it can be stated that the higher γ results in quicker initiation of liquefaction, i.e. the condition $r_u = 1$ is attained in smaller number of cycles (N).

Figure 2b presents the variation in maximum r_u in each cycle with N at different γ . It shows that with the increase in γ , i.e. from 0.045% to 0.75%, the liquefaction resistance decreases. r_u values were observed to be nearly 0.2 and 0.55 for $\gamma = 0.045\%$ and 0.075%, respectively, whereas r_u attains equal to 1 for γ range 0.15–0.75% at $N = 40$ cycles. This is attributed to the higher CSR developed at successive increment of shear strain amplitude (owing to larger deviatoric stress applied at each stage), as presented in Table 4. The higher values of the CSR at first cycle, consequently leads to higher value of r_u , thereby leading to quicker development on liquefaction condition at smaller number of cycles. Tests were also conducted at $\gamma > 0.75\%$ as listed in Table 2, which showed that BS specimen, prepared at $D_r = 30\%$ and subjected to $\sigma'_c = 100$ kPa, attains $r_u \geq 0.9$, indicating the onset of liquefaction at the very 1st cycle itself. It can also be noted that more number of cycles (N) are required to initiate liquefaction for soil specimen subjected to $\gamma < 0.60\%$. Similar responses were observed for the specimens prepared at $D_r = 60\%$ and 90%, subjected to $\sigma'_c = 50$ kPa and 150 kPa.

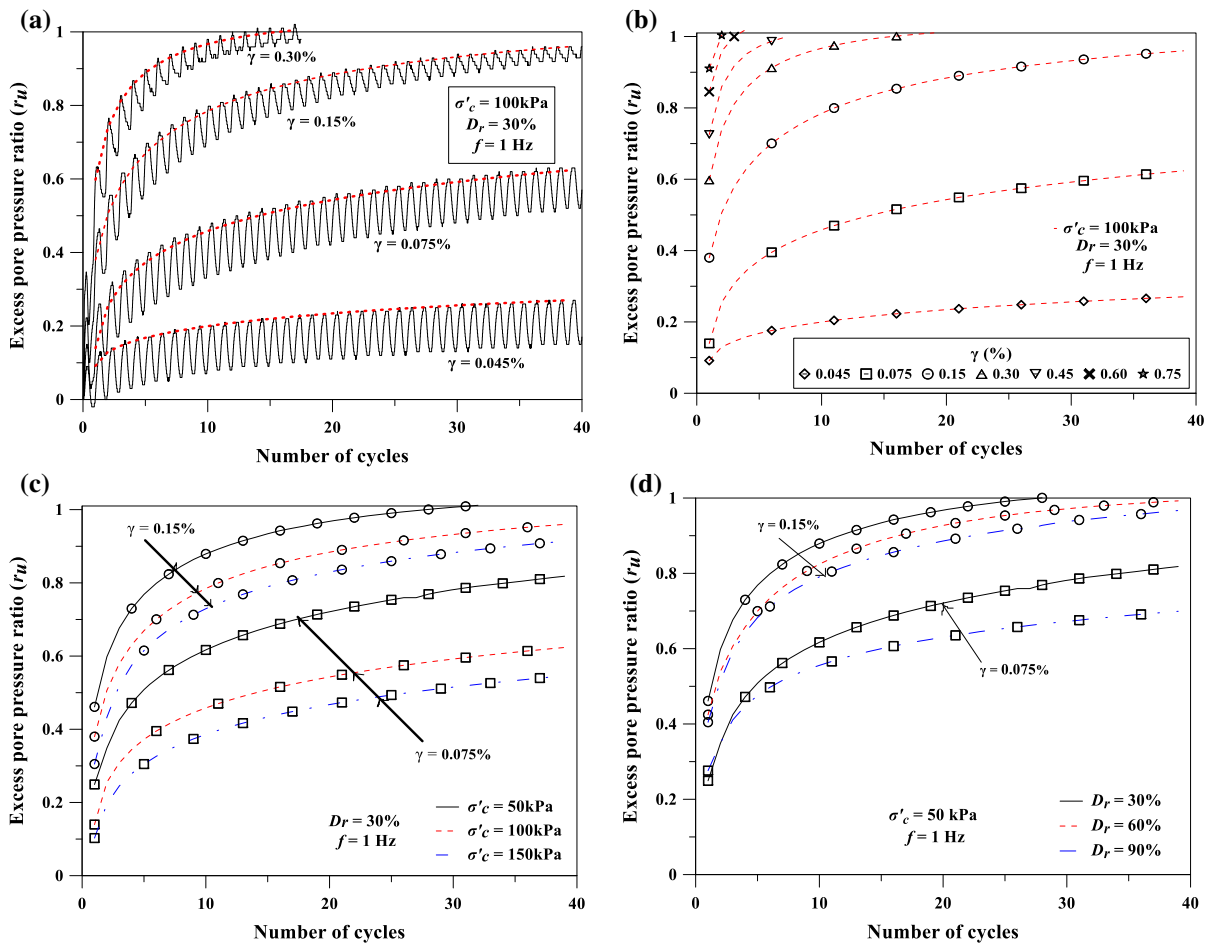


Fig. 2 Variation of **a** r_u with N from a cyclic strain-controlled tests, **b** maximum r_u with N at different γ ; **c** maximum r_u with N at different σ'_c and γ ; **d** maximum r_u with N at different D_r and γ

Figure 2c presents the variations of r_u at different σ'_c for BS specimens prepared at $D_r = 30\%$, and subjected to γ equal to 0.075% and 0.15%. For $\gamma = 0.075\%$, maximum r_u value is 0.8 at $\sigma'_c = 50$ kPa, maximum $r_u = 0.53$ at $\sigma'_c = 150$ kPa; whereas, for $\gamma = 0.15\%$, the maximum r_u value reached 1 at 30 cycles for $\sigma'_c = 50$ kPa, while $r_u = 0.90$ at 30 cycles for $\sigma'_c = 150$ kPa. Thus, the figure indicates that for a given γ (say for 0.15%) and N , r_u values decreases with increase in σ'_c . It also shows that for identical N and σ'_c (say for 100 kPa), the tendency of the specimen to liquefy increases with increase of γ . It is seen that, for a given γ (e.g. 0.15%) and N , CSR values for first cycle decreased with increase in σ'_c , thereby resulting in the suppression of r_u ; whereas, for identical N and σ'_c (e.g. 100 kPa), CSR values for first cycle increased with increase in γ , thereby resulting in the enhancement of

r_u . The same is further clarified in the data presented in Table 4.

Figure 2d illustrates the variation in r_u for test specimens prepared at different D_r i.e. 30%, 60% and 90%, and tested at $\sigma'_c = 50$ kPa with γ of 0.075% and 0.15%. It reflects that the r_u decreases with the increase of D_r subjected to a particular γ and σ'_c . At $\gamma = 0.075\%$ and at 40 cycles, the BS specimen shows maximum $r_u = 0.8$ and 0.7, for $D_r = 30\%$ and 90%, respectively, whereas at $\gamma = 0.15\%$, the maximum r_u was observed to be 1.0 (at 32 cycles) and 0.9 (at 40 cycles), for $D_r = 30\%$ and 90%, respectively. Therefore, it can be stated that the initiation of liquefaction is significantly affected by D_r as well as γ . It is also seen that for any constant γ (0.075% or 0.15%), the r_u is nearly same at first cycles for all three D_r .

Table 4 Parameters of the strain controlled cyclic triaxial tests

D_r (%)	σ'_c (kPa)	Parameters	γ (%)								
			0.015	0.045	0.075	0.15	0.30	0.45	0.60	0.75	
30	50	σ_d (kPa)	6	15	25	30	41	41	49	48	
		CSR	0.06	0.15	0.25	0.30	0.41	0.41	0.49	0.48	
		N_L	NL	NL	NL	16	4	4	2	1	
		r_u	0.08	0.54	0.8	1	1	1	1	1	
	100	σ_d (kPa)		25	35	57	71	79	82	95	
		CSR		0.13	0.18	0.29	0.36	0.40	0.41	0.48	
		N_L		NL	NL	NL	16	7	4	1	
		r_u		0.27	0.62	0.96	1	1	1	1	
	150	σ_d (kPa)		31	46	66	96	105	112	138	
		CSR		0.1	0.15	0.22	0.32	0.35	0.38	0.46	
		N_L		NL	NL	NL	18	9	5	3	
		r_u		0.25	0.55	0.91	1	1	1	1	
60	50	σ_d (kPa)	9.6			41			47		
		CSR	0.096			0.41			0.47		
		N_L	NL			40			3		
		r_u	0.07			0.99			1		
	100	σ_d (kPa)	13			64			95		
		CSR	0.065			0.32			0.47		
		N_L	NL			NL			7		
		r_u	0.045			0.75			1		
	150	σ_d (kPa)	12			85			117		
		CSR	0.04			0.28			0.39		
		N_L	NL			NL			8		
		r_u	0.015			0.68			1		
90	50	σ_d (kPa)		20	32	36	49	66	83	85	
		CSR		0.20	0.32	0.36	0.49	0.66	0.83	0.85	
		N_L		NL	NL	NL	10	3	1	1	
		r_u		0.47	0.70	0.97	1	1	1	1	
	100	σ_d (kPa)		34	43	58	87	90	103		
		CSR		0.17	0.22	0.29	0.44	0.45	0.52		
		N_L		NL	NL	NL	28	12	4		
		r_u		0.35	0.61	0.86	1	1	1		
	150	σ_d (kPa)		40	56	73	106	120	130	170	
		CSR		0.14	0.19	0.24	0.35	0.40	0.44	0.57	
		N_L		NL	NL	NL	32	20	8	7	
		r_u		0.30	0.52	0.89	1	1	1	1	

N_L is number of cycles to liquefy the specimen; NL is not liquefied in 40 cycles; σ_d (kPa) is deviatoric stress employed on the specimens at first cycle for given γ ; CSR is cyclic stress ratio at first cycle; r_u is excess PWP ratio

5.1.2 Variation of Shear Stress and CSR at Different γ , σ'_c and D_r

Figure 3 shows the variations in shear stress ($\tau = \sigma_d/2$) with the number of cycles (N) at different γ (Fig. 3a), σ'_c (Fig. 3b) and D_r (Fig. 3c). The figure also shows the same in terms of cyclic stress ratio ($CSR = \sigma_d/$

$2\sigma'_c$). Figure 3a shows the variations in shear stress (τ) and CSR with N at different γ , for constant $\sigma'_c = 50$ kPa and $D_r = 30\%$. The decrease in shear stress reflects the strength reduction of soil with increasing numbers of loading cycles. The rate of reduction in shear stress is higher at higher γ , which is attributed to the higher magnitude of excess PWP developed in the

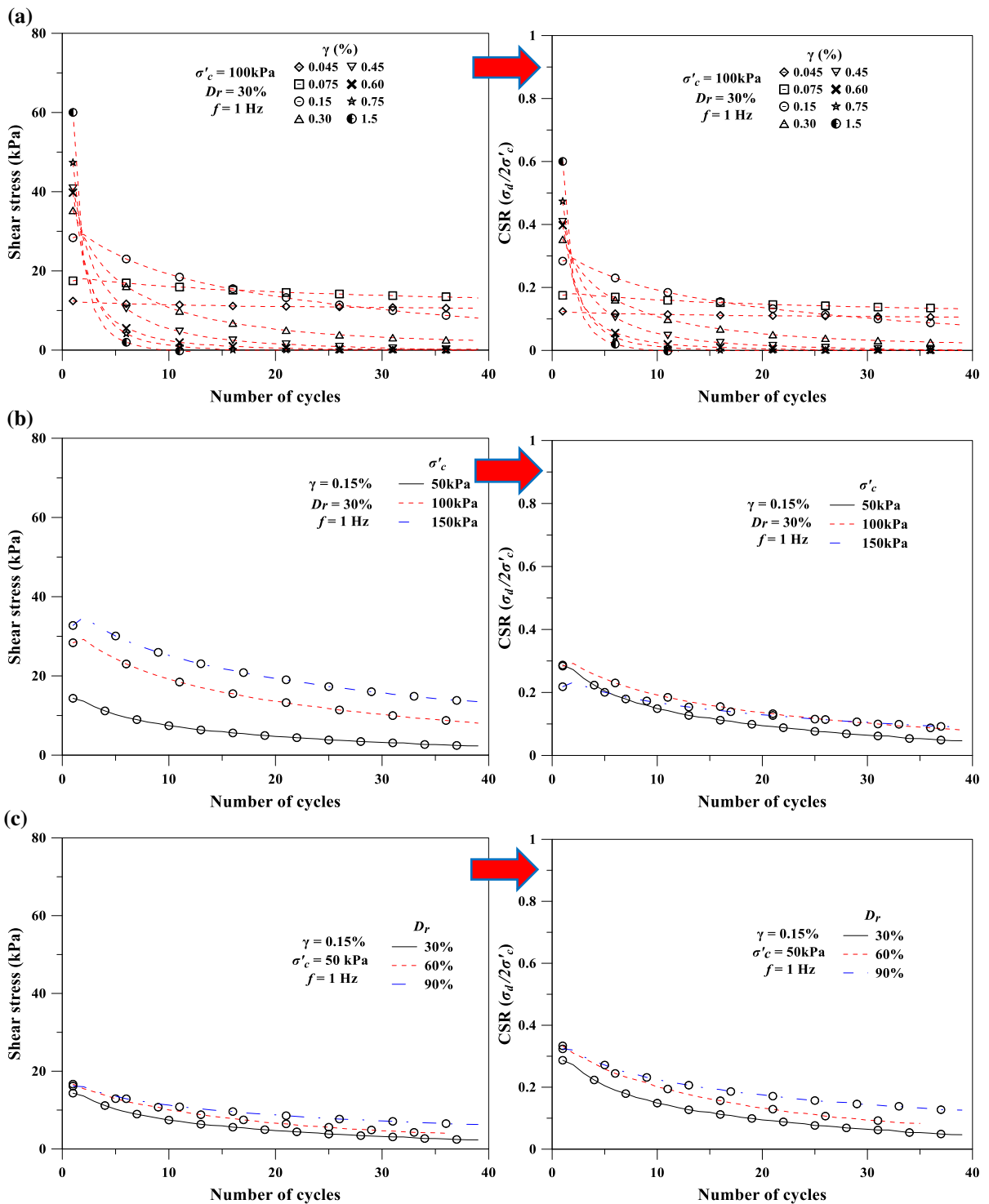


Fig. 3 Variation of shear stress and CSR with N at different **a** γ , **b** σ'_c , **c** D_r

soil specimen at higher γ . Figure 3a also illustrates that for the first cycle, the shear stress and CSR is significantly higher for higher γ , and the same decreased continuously with subsequent loading cycles and finally reaches to zero in case of liquefaction of the soil. Figure 3b presents the variations in shear stress (τ) with N at different σ'_c for constant $D_r = 30\%$ and $\gamma = 0.15\%$. τ was observed to be nearly 15 kPa, 30 kPa and 35 kPa for 1st cycles at $\sigma'_c = 50$ kPa, 100 kPa and 150 kPa, respectively, whereas CSR was found to be nearly 0.3, 0.3 and 0.22 for 1st cycles at $\sigma'_c = 50$ kPa, 100 kPa and 150 kPa, respectively. Shear stress ($\tau = \sigma_d/2$) developed in the soil specimen is directly proportional to σ'_c , whereas CSR ($= \sigma_d/2\sigma'_c$) depends on both σ_d and σ'_c . Therefore, it can be stated that for $D_r = 30\%$ and $\gamma = 0.15\%$, higher σ'_c imparts higher $\tau (= \sigma_d/2)$ in the soil specimens, whereas the CSR ($= \sigma_d/2\sigma'_c$) is negligibly affected by its variation.

Figure 3c presents the variations in τ and CSR with N , at different D_r for constant $\sigma'_c = 50$ kPa and $\gamma = 0.15\%$. τ is found to be nearly 14 kPa, 16 kPa and 16 kPa for 1st cycles at $D_r = 30\%$, 60% and 90%, respectively, whereas the CSR is found to be nearly 0.29, 0.33 and 0.33 for 1st cycles at $D_r = 30\%$, 60% and 90%, respectively. $\tau (= \sigma_d/2)$ in the soil specimens depend on σ'_c , which is constant for all D_r , and hence either σ_d or τ is almost independent of D_r (as reported in Fig. 3c). However, small changes in τ and CSR is observed which may be due to the changes in the particle adjustments and consequent irregularities in the excess PWP during cyclic loading. Moreover, it can be stated that both τ and CSR are negligibly affected by D_r , for a constant σ'_c (50 kPa) and γ (0.15%).

CSR generally used to define the cyclic strength of soil, is an index to manifest the stresses applied on the soil specimens against σ'_c in stress-controlled loading. In strain-controlled loading, the amount of stress applied on the soil specimens, at particular values of σ'_c and γ , is evaluated in terms of CSR. The maximum CSR developed at the first cycle, for different γ , D_r and σ'_c are presented in Table 4. It is observed that CSR increases with the increase in γ for $D_r = 30\%$ and $\sigma'_c = 50$ kPa, because the developed deviator stresses (σ_d) in first cycle increases with the increase in displacement rate (γ). Table 4 also presents that the number of cycles required for the specimen to attain the initiation of liquefaction (N_L), corresponding to

particular magnitude of γ and developed CSR. It is seen that with the increase in CSR, the liquefaction resistance of BS specimen decreased, as reflected by the attained values of r_u . The CSR values decreases with the increase of σ'_c (from 50 to 150 kPa) for constant D_r and γ . Similar results are observed for $\sigma'_c = 100$ kPa and 150 kPa (Table 4). The results obtained for $D_r = 60\%$ and 90%, and $\sigma'_c = 50$ –150 kPa were similar to $D_r = 30\%$ and $\sigma'_c = 50$ –150 kPa, as well as the reasoning resemble to the latter. For all D_r and σ'_c , it is observed that the developed deviator stress (σ_d) is much higher than the initial σ'_c at $\gamma > 0.75\%$, thereby the evaluated CSR ($= \sigma_d/2\sigma'_c$) becomes equal to or larger than 0.5.

Based on Table 4, the developed CSR attains a value of 0.5 with $r_u = 1$ at almost $\gamma \approx 1.0\%$, which can be considered as a limiting value of γ ($\approx 1.0\%$) to attain the onset of liquefaction. Beyond this limiting γ , when CSR becomes larger than 0.5, the specimen is not able to resist even a single loading cycle, and the soil column was observed to collapse/fail because of extensive increase in excess PWP i.e. nearly equal to or larger than the initial σ'_c . Kramer (1996) reported that the soil shows flow failure criteria when σ'_c is smaller than the applied stress. Thus, from the present study, it can be observed that the BS specimen shows initiation of liquefaction for different D_r and σ'_c , when the CSR reached nearly equal to 0.5.

5.2 Stress-Controlled Approach

Stress-controlled regular excitation is a simplified representation of irregular excitation, wherein the equivalent number of regular loading cycles is used to represent the latter. In the present study, the methodology proposed by Seed and Idriss (1970) was used to evaluate the regular deviatoric stress loading for CSR = 0.05–0.4, which was applied on BS soil specimens for the stress-controlled laboratory tests. Test results were presented in terms of accumulation of γ and generation of excess pore water pressure (u_e), which is further represented as excess PWP ratio ($r_u = u_e/\sigma'_c$). Typical plots of the responses obtained from stress-controlled tests are presented in Fig. 4a–d. Figure 4a shows the variations in σ_d with mean effective at CSR = 0.1, 0.2, 0.3 and 0.4, for the specimens prepared at $D_r = 60\%$ and $\sigma'_c = 100$ kPa. It illustrates that the σ_d applied on the soil specimens increases with the increase of CSR, which lead to the

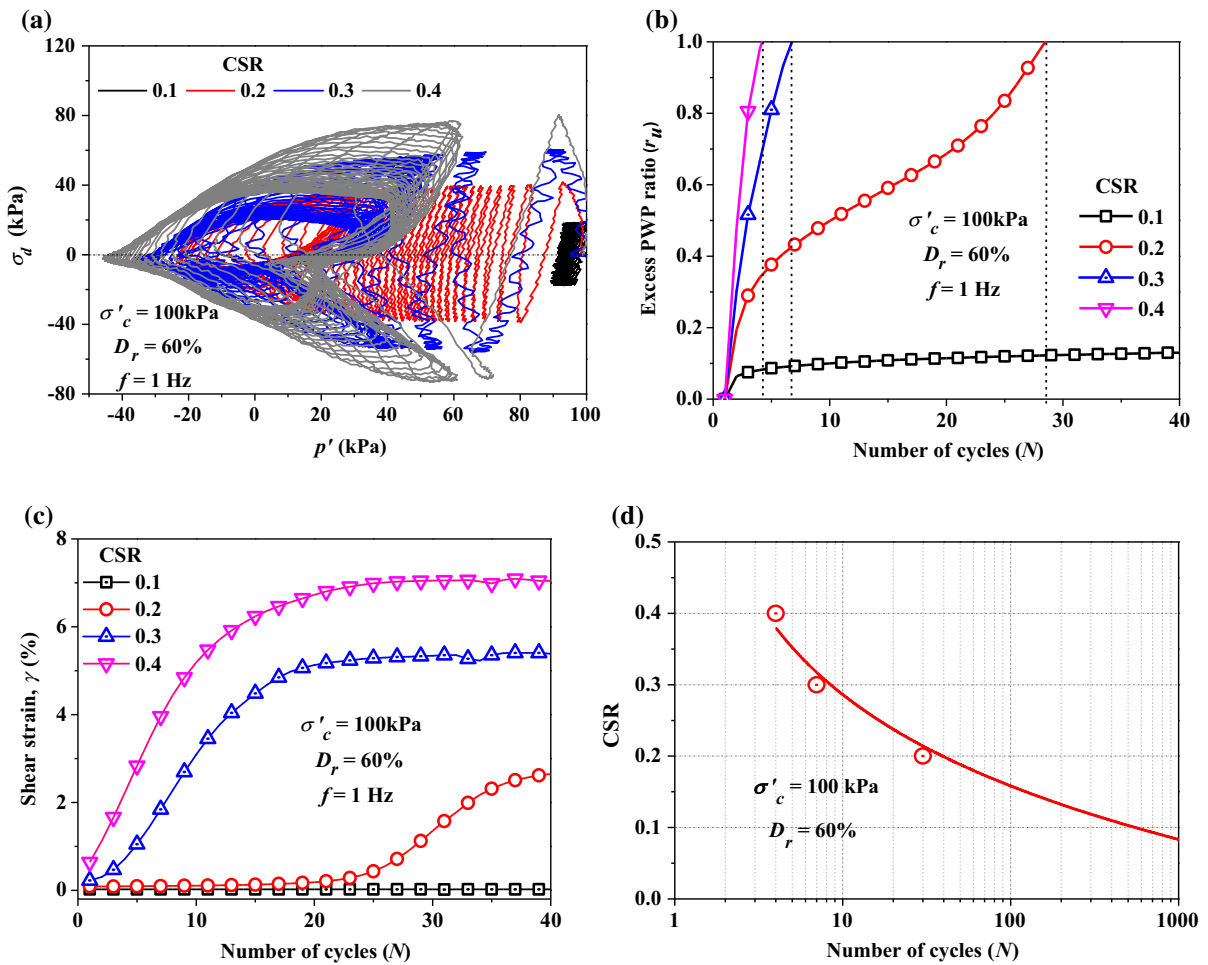


Fig. 4 a Stress path plot at different CSR; b variation in r_u with number of cycles at CSR; c variations in γ with number of cycles at different CSR; d variation of CSR with number of loading cycles, during stress-controlled test

quick liquefaction of soil. It is also seen that the effective stress path becomes tapered when initiation of liquefaction occurred in the soil specimen. The number of cycles (N) of repetitive load, corresponding to the applied CSR, is responsible for the development of r_u (shown in Fig. 4b) and accumulation of γ (presented in Fig. 4c). Figure 4b presents the variations in r_u with N at different CSR. It was noticed that the specimen subjected to CSR = 0.1 does not show initiation of liquefaction even up to 500 cycles which is due to significantly lower amount of strain accumulation. However, specimens subjected to other values of CSR = 0.2, 0.3 and 0.4 exhibited the initiation of liquefaction ($r_u = 1$) at $N = 29, 7$ and 4 , respectively. For the sake of comparison with other CSR values, the same has been presented up to 40

cycles (Fig. 4b, c). Figure 4c reflects the variations in accumulated γ with N at different CSR. It shows that γ reached 1.0%, 2.0% and 2.5% at CSR values 0.2, 0.3 and 0.4, respectively when BS specimens shows $r_u = 1$.

Figure 4d shows the variations in CSR with number of cycles (N) at $D_r = 60\%$ and $\sigma'_c = 100\text{ kPa}$. It is seen that the BS specimen shows liquefaction at $N = 4, 7$ and 29 for CSR = 0.4, 0.3 and 0.2, respectively, whereas at CSR = 0.1, no liquefaction was observed even till 500 cycles (hence, the same is not represented in the figure). Thus, it can be stated that the BS specimen liquefies in smaller number of cycles when subjected to higher CSR. This is attributed to the higher deviatoric stress applied on the specimen at higher CSR. Several other tests have been conducted at

different D_r , σ'_c and CSR, and the results are presented in the following sections.

5.2.1 Variation of r_u and γ with Cyclic Loading at Different σ'_c and CSR

Figure 5a presents the variation in r_u of BS specimens ($D_r = 30\%$; $\sigma'_c = 50, 100$ and 200 kPa) for different CSR ($\sigma_d/2\sigma'_c$: 0.05–0.3). The specimens subjected to CSR = 0.2 was found to exhibit onset of liquefaction at $N = 10, 4$ and 3 for $\sigma'_c = 50, 100$ and 200 kPa, respectively; while, at CSR = 0.3, the onset is portrayed at $N = 2$, subjected to effective confining stresses 50 and 100 kPa, respectively. Figure 5a illustrates that specimens subjected to $\sigma'_c = 50$ kPa, and CSR = 0.05 and 0.1, the signs of liquefaction was not pertinent till 100 cycles. When the specimen was subjected to CSR = 0.1, the onset was manifested at 122nd and 62nd loading cycle for $\sigma'_c = 100$ and 200 kPa, respectively. Thus, it is observed that the attainment of liquefaction in BS specimens is profoundly influenced by the increment of σ'_c , attributed to the simultaneous enhancement in γ and σ_d . Similar note have been reported in available literature (Simatupang and Okamura 2017).

For BS specimens prepared at $D_r = 30\%$ and subjected to different σ'_c , Fig. 5b portrays the shear strain accumulation under different CSR (0.05–0.3). It reveals that for CSR = 0.2, at $\sigma'_c = 50, 100$ and 200 kPa, the accumulated shear strain at the attainment of liquefaction was 0.45%, 2.5% and 6.8%, respectively; while for CSR = 0.3, the accumulated

shear strain was observe to be larger than 1%, when subjected to $\sigma'_c = 50$ and 100 kPa. It is also illustrated that for specimens subjected to $\sigma'_c = 50$ kPa, the scenario of liquefaction did not arise when subjected to CSR = 0.05 and 0.1, and that the accumulated shear strain was approximately 0.02% till 500 cycles. The accumulated γ was 0.5% and 1.5% as liquefaction initiated in the samples (prepared at $D_r = 30\%$ and subjected to CSR = 0.1) at 122nd and 62nd loading cycles, when subjected to $\sigma'_c = 100$ and 200 kPa, respectively. Thus, it can be stated that for the same CSR, σ_d and γ increases substantially with the increase in σ'_c and, consequently requires smaller number of cycles for the onset of liquefaction. Experiences from the past earthquakes have revealed that liquefaction had mainly occurred at shallow depths (i.e. < 15 m), while the laboratory experiments have made it evident that the liquefaction resistance of soil depends upon the confining stress along with other testing conditions (Seed and Idriss 1970; Elgamal et al. 1996). Tumi (1983) and Govindaraju (2005) reported that the liquefaction resistance of sandy soil decreases with the increase of σ'_c using stress-controlled approach, while the same increases during a strain-controlled approach. Experimental and numerical investigations also revealed that the liquefaction may occur at bottom layer or at depths larger than 15 m depending upon peak ground acceleration and soil conditions (Seed and Idriss 1970; Elgamal et al. 1996; Byrne et al. 2004; Sreng et al. 2015; Qu et al. 2016). Therefore, the results presented in this section, can be used as an

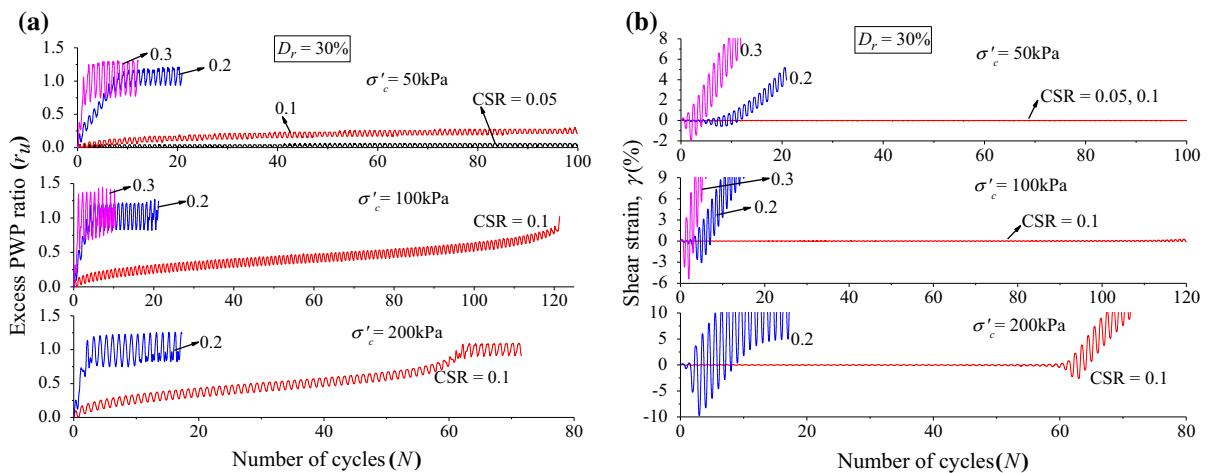


Fig. 5 Variation of **a** r_u with N , **b** γ with N , at different σ'_c and CSR for $D_r = 30\%$

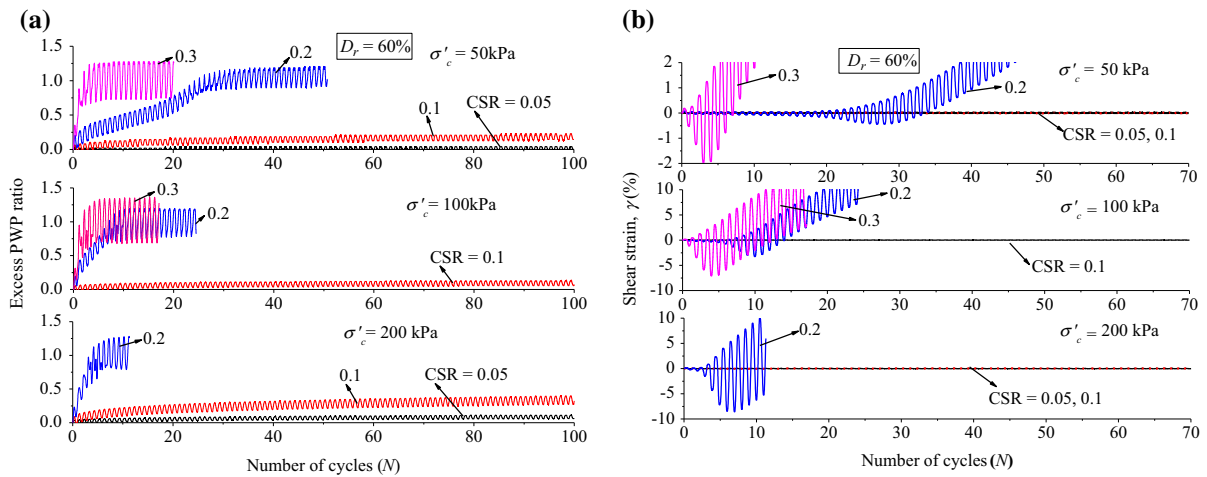


Fig. 6 Variation of **a** r_u with N , **b** γ with N , at different σ'_c and CSR at $D_r = 60\%$

artefact to understand the behaviour of sand specimens subjected to regular cyclic stress excitations.

Figure 6a presents the response of BS soil specimens for $D_r = 60\%$ at $\sigma'_c = 50, 100$ and 200 kPa. The specimens at each σ'_c were subjected to different cyclic stress amplitudes ($CSR = 0.5–3$). It is observed that the specimens subjected to confining stress $50, 100$ and 200 kPa, and tested at $CSR = 0.2$ portray initiation of liquefaction at $N = 30, 9$ and 3 , when s respectively; whereas, for $CSR = 0.3$, the liquefaction is reflected at $N = 3$ and 2 for confining stress 50 and 100 kPa, respectively. Liquefaction was not reported at $CSR = 0.05$ and 0.1 even in the 500 th cycle. It was also observed that the liquefaction resistance decreases with the increase of σ'_c for any particular CSR (for example, $CSR = 0.2$), thus indicating the stress level dependency, since σ_d increases with the increase in σ'_c .

Figure 6b illustrates the shear strain accumulation during cyclic loading at $D_r = 60\%$ and tested for CSR range $0.05–0.3$. It reflects that, for $CSR = 0.2$, the γ was larger than 0.5% when the initiation of liquefaction occurred, for all the magnitude of σ'_c ($50, 100$ and 200 kPa); whereas, for $CSR = 0.3$, the γ was 0.75% for both $\sigma'_c = 50$ and 100 kPa. It also shows that the liquefaction was not attained at $CSR = 0.05$ and 0.1 , and the accumulated shear strain was approximately 0.02% . For same CSR, it is seen that with the increase in σ'_c , σ_d increases substantially, and consequently, the number of cycles required for the onset of liquefaction reduces. The summary of results regarding the number of cycles required and the corresponding shear strain

generated at the onset of liquefaction, obtained for different σ'_c , is presented in Table 5.

Table 5 clearly shows that, for a particular D_r (say, 60%), the liquefaction resistance of soil decreases with increase in CSR and σ'_c . It also shows that the initiation of liquefaction occurred at different confining depth (i.e. represented by the increasing magnitudes of σ'_c), when accumulation of γ exceeded 0.5% . Thus, based on the stress-controlled tests, it can be stated that the accumulation of γ is also one of the major contributory factor along with the generation of excess PWP for designating the initiation of liquefaction in saturated sand.

5.2.2 Variation of r_u and γ with Cyclic Loading at Different D_r and CSR

Figure 7a presents the behaviour of saturated BS specimens, in terms of variations in r_u and γ , prepared at different D_r , subjected to varying CSR (i.e. $0.05–0.3$) for regular excitation of 100 cycles. The tests have been conducted up to 500 cycles for $CSR = 0.05$ and 0.1 . It was observed that specimens prepared at any particular D_r , and subjected to low magnitude CSR (for example, $CSR = 0.05$ and 0.1), does not exhibit liquefaction even in the 500 th cycle; whereas, specimens subjected to higher CSR magnitudes (for example, $CSR = 0.2$ and 0.3) manifested the occurrence of liquefaction. Figure 7a illustrates that at $D_r = 30\%$ and $\sigma'_c = 50$ kPa, the specimens at CSR values 0.2 and 0.3 liquefied at $N = 10$ and 2 , respectively. Similar behaviour is portrayed at other

Table 5 Summary of results regarding the number of cycles and shear strain generated at the onset of liquefaction for BS subjected to regular excitation and at different σ'_c

D_r (%)	σ'_c (kPa)	Number of cycles (N) to liquefaction and shear strain (γ)	CSR			
			0.05	0.1	0.2	0.3
60	50	N	NL	NL	30	3
		γ (%)	0.02	0.02	0.5	0.75
	100	N	NL	NL	10	2
		γ (%)	0.02	0.02	0.75	0.75
200	N	NL	627	4		
	γ (%)	0.02	0.5	0.75		

NL no liquefaction till 500 cycles

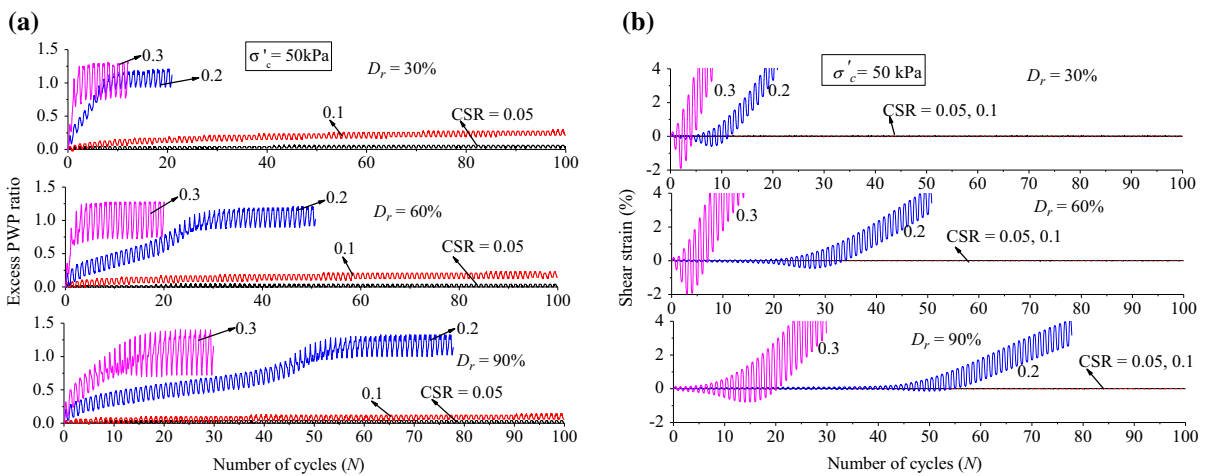


Fig. 7 Variation of **a** r_u with N , **b** γ with N , at different D_r and CSR at $\sigma'_c = 50$ kPa

magnitudes of relative densities. It can be observed that the number of cycles required to exhibit liquefaction increases with the increase in D_r of the specimen. In other words, it can be stated that the liquefaction potential decreases with increasing D_r or, compactness of the soil.

Figure 7b presents the response of BS soil specimens prepared at $D_r = 30\%$, 60% and 90% at $\sigma'_c = 50$ kPa. The specimen at different D_r was subjected to different cyclic stress amplitudes defined by different CSR values (0.05–0.3). It is observed that for $D_r = 30\%$, the specimen with CSR values of 0.05 and 0.1 exhibit substantially low magnitudes of shear strain. It can also be noticed that at $D_r = 30\%$, 60% and 90% , subjected to CSR = 0.2, BS portrays onset of liquefaction at $N \sim 10$, 30 and 50 cycles,

respectively, when the corresponding shear strain reaches nearly 0.5%. For samples prepared at $D_r = 30\%$, 60% and 90% , $\gamma \geq 0.5\%$ was observed at CSR = 0.3 when the initiation of liquefaction observed at $N \sim 2$, 3 and 10 cycles, respectively. The summary of the outcomes from the tests conducted at different D_r are presented in Table 6. Similar to the Table 5, it can also be stated that the initiation of liquefaction occurred at different D_r , when the accumulation of γ exceeded 0.5%.

Based on the variation of CSR values, Fig. 8 presents the nutshell of the number of loading cycles required to attain the initiation of liquefaction (N_L) in the BS specimens (prepared at $D_r = 30\text{--}90\%$ and subjected to $\sigma'_c = 100$ kPa). It shows that for any particular CSR (e.g. CSR = 0.2), the increase in

Table 6 Summary of results regarding the number of cycles and shear strain generated at the onset of liquefaction for BS subjected to regular excitation and prepared at different D_r

σ'_c (kPa)	D_r (%)	Number of cycles (N) to liquefaction and shear strain (γ)	CSR			
			0.05	0.1	0.2	0.3
50	30	N	NL	NL	10	2
		γ (%)	0.02	0.02	0.6	0.75
	60	N	NL	NL	30	3
		γ (%)	0.02	0.02	0.5	0.75
	90	N	NL	NL	30	3
		γ (%)	0.02	0.02	0.5	0.5

NL no liquefaction till 500 cycles

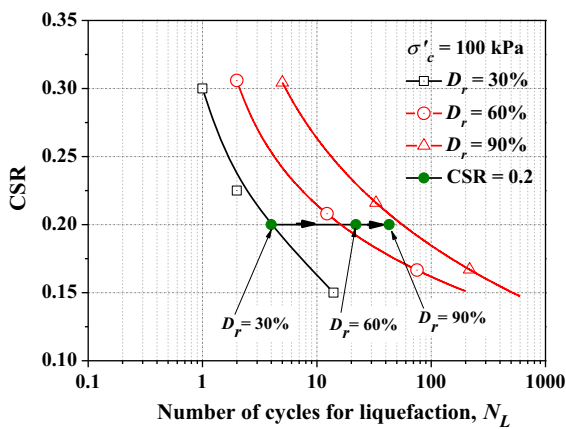


Fig. 8 Variation of CSR with N_L (Kumar et al. 2018a, b)

relative density ($D_r = 30\text{--}90\%$) results in the increase in liquefaction resistance. As a corollary, for any particular D_r , an increase in the CSR (0.15–0.3) leads to the decrement in the liquefaction resistance. Thus, it can be stated that even at low shaking (represented by low CSR), saturated BS specimens in their loose state is sufficiently vulnerable to liquefaction, while they are relatively resilient at their higher relative densities.

5.3 Comparative Results of Strain-Controlled and Stress-Controlled Tests

Figures 9, 10 and 11 present the combined input and output response for strain-controlled and stress-controlled tests conducted at different shear strain (γ) and CSR. Figure 9a represents the input of strain-controlled conducted at $\gamma = 0.045\%$ and stress-controlled test conducted at CSR = 0.1 (approximate deviatoric

stress of 20 kPa applied on the specimen), while Fig. 9b shows the corresponding outputs., respectively. It can be seen from Fig. 9b that the outcome of strain controlled test illustrates the development of deviatoric stress of approximately 25 kPa and $r_u = 0.2$ at the end of 40 cycles corresponding to $\gamma = 0.045\%$. Corresponding to the stress-controlled test subjected to CSR = 0.1, at the end of 120 cycles, the shear strain of approximately 0.35% and $r_u = 0.9$ is developed. It is also noticed that at the end of 40 cycles, the r_u obtained from stress-controlled approach is significantly higher (nearly twice) than that obtained from the strain-controlled approach. Since the development of pore water pressure significantly affects dynamic properties (shear modulus and damping ratio) and strength of the soils, it can be justified that the dynamic response of soils also depends on the testing methodology. Several researchers have reported about the evaluation of dynamic properties from stress-controlled approach based on different loading–unloading cycles (Sitharam et al. 2012; Kumar et al. 2015).

Similar response is obtained at a different set of shear strain and CSR ($\gamma = 0.075\%$ and CSR = 0.2), as presented in Fig. 10. It can be seen that although the stress generated in strain-controlled tests and that applied for stress-controlled test is approximately 40 kPa, the variation in r_u is entirely different from both the approaches, similar to that obtained in Fig. 9. Thus, based on Figs. 9 and 10, it can be stated that the dynamic properties evaluated from either of the approaches will be different and requires proper insight and justification for their application to practical geotechnical problems. Figure 11 depicts the

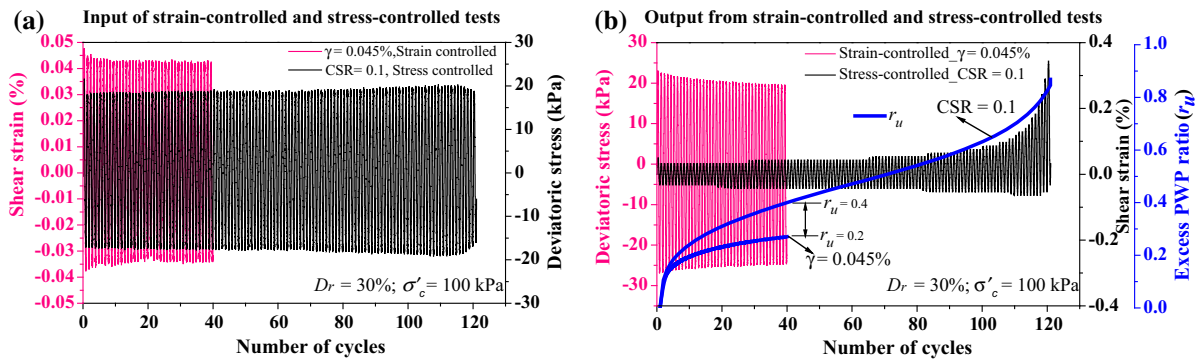


Fig. 9 a Input and b output of strain- and stress-controlled at $\gamma = 0.045\%$ and $CSR = 0.1$

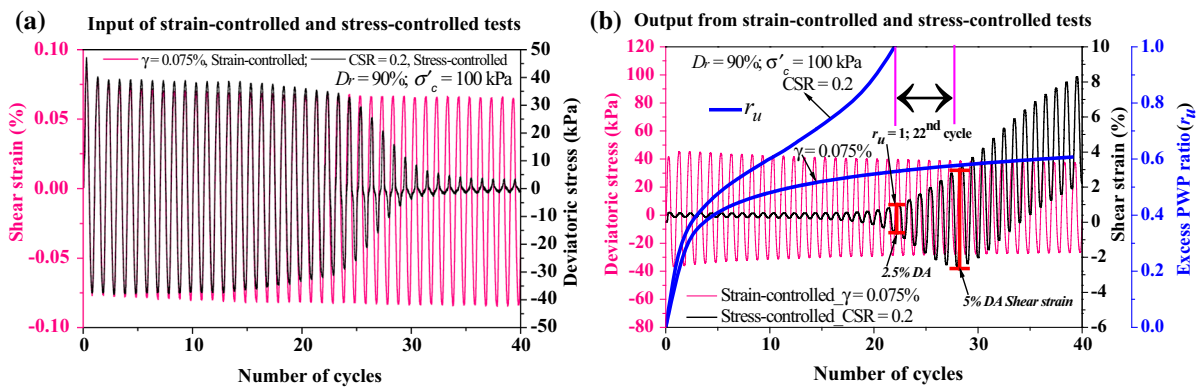


Fig. 10 a Input and b output of strain- and stress-controlled at $\gamma = 0.075\%$ and $CSR = 0.2$

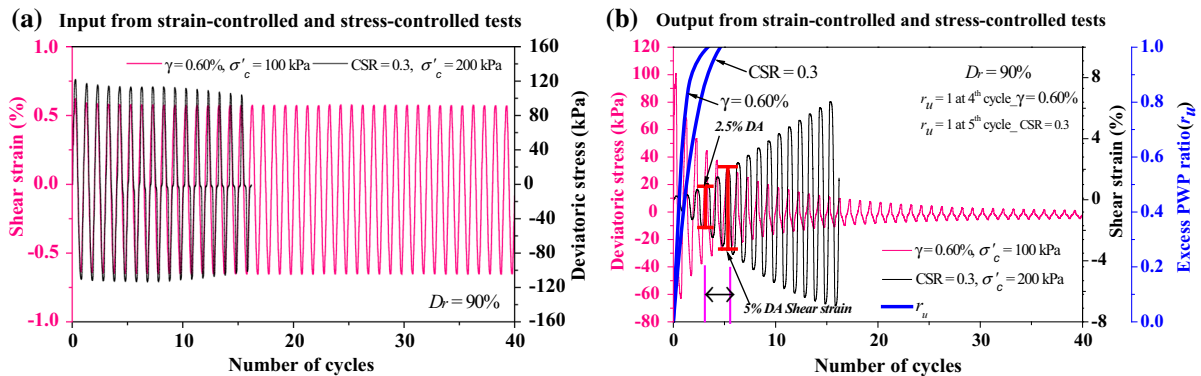


Fig. 11 a Input and b output of strain- and stress-controlled at $\gamma = 0.60\%$ and $CSR = 0.3$

input (Fig. 11a) and output (Fig. 11b) responses for strain-controlled and stress-controlled tests, at $\gamma = 0.60\%$ and $CSR = 0.3$, respectively. It is seen that the variations of excess PWP ratio is nearly similar and specimens shows $r_u = 1$ at 4th and 5th cycles with strain and stress-controlled approach, respectively. Moreover, it is seen from Figs. 9, 10

and 11 that the excess PWP ratio at first loading–unloading cycle is nearly same from both strain and stress-controlled approaches. Hence, it can be stated that the dynamic properties and the strength of the soil would not be significantly different at first loading–unloading cycle from either types of test procedures. It has also been seen from Figs. 9 and 10 that the

variations in excess PWP ratio based on stress-controlled approach is significantly higher than the strain-controlled approach, which is attributed to the accumulation of higher magnitude of shear strains with the loading cycles in stress-controlled approach. Therefore, it can be stated that the shear strain accumulation along with the PWP generation during stress-controlled dynamic loading quicken the initiation of liquefaction (i.e. requires smaller number of loading cycles) in comparison to that required in strain-controlled loading. The simultaneous accumulation of shear strain during stress-controlled loading along with the progressive development of excess PWP renders stress-controlled approach to be a better option to evaluate the liquefaction potential of soil; whereas, to evaluate the dynamic properties, strain-controlled approach can be regarded as the suitable option, since the dynamic properties at any particular shear strain can be accurately estimated.

6 Dynamic Soil Properties

The evaluation of dynamic properties of soil has been generally carried out by strain-controlled approach, since amplitudes remain constant in both compression and extension phases; and hence the dynamic properties are evaluated at a constant shear strain for any loading cycle. Figure 12 represents a typical hysteresis plot obtained from strain- and stress-controlled test. Figure 12a illustrates that during strain-controlled tests, for successive cycles, the slope and area of

hysteresis loops gradually diminishes with the loading cycles. Thus, for strain-controlled approach, the dynamic properties of soil are still liable to change even though constant amplitudes in compression and extension phases are effective. Figure 12b illustrates the stress–strain response obtained from stress-controlled approach, where strain amplitudes are not constant in compression and extension phases. Apart from strain, even though the tests is stress-controlled, the generated shear stresses gradually reduces with the loading cycles, attributed to the development of pore-pressures during the test.

The development of different magnitude of strains during compression and extension phases, in stress-controlled tests, leads to inaccurate estimation of stiffness degradation (Sitharam et al. 2012). The stress-controlled test can be stated as a better representation to simulate the field liquefaction condition where the specimen undergoes simultaneous accumulation of PWP and shear strain subjected to the application of constant amplitude shear stresses. For the evaluation of dynamic soil properties, the methodology reported in Kumar et al. (2017a, b) has been used for both strain-controlled and stress-controlled results (Fig. 13).

Figure 14 shows the variation of shear modulus and damping ratio obtained from strain-controlled and stress-controlled approaches at different magnitudes of constant shear strain amplitudes and CSR, respectively. For the evaluation of shear modulus and damping ratio from strain-controlled tests, the first cycle of various loading sequences was selected (as

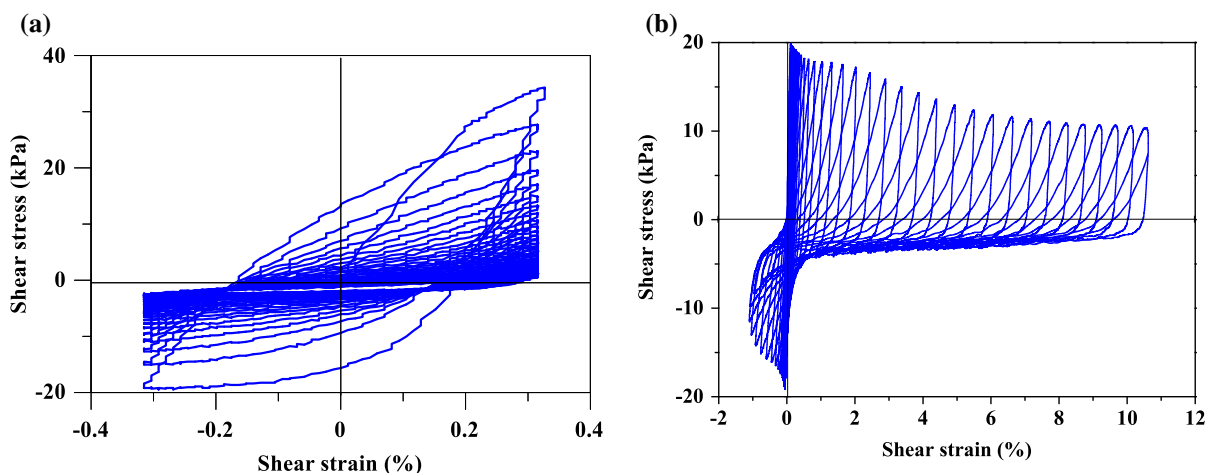
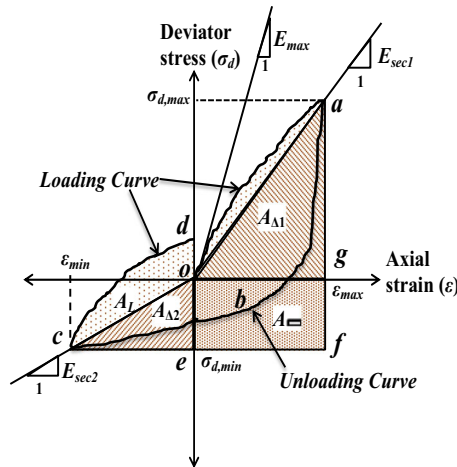


Fig. 12 Typical stress–strain response during **a** strain and **b** stress-controlled loading



$$E_{sec,a} = \frac{E_{sec1} + E_{sec2}}{2}$$

$$G_a = E_{sec,a} / [2(1 + \nu)]$$

$$\gamma = (1 + \nu)\epsilon$$

$$D^\# = \frac{1}{\pi} \times \frac{A_{L(o-a-b-c-d)}}{A_{\Delta1} + A_{\Delta2} + A_{\square}}$$

Fig. 13 Method to evaluate the dynamic soil properties (Kumar et al. 2017a, b)

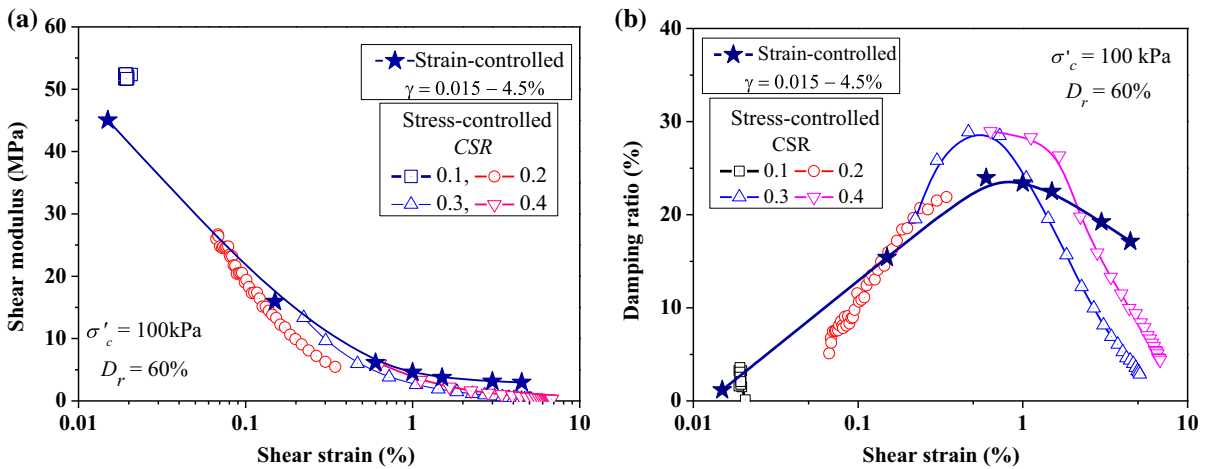


Fig. 14 Variation of a shear modulus, b damping ratio obtained from strain and stress-controlled loading

peak shear strain remains constant for a particular test), whereas, successive loading–unloading cycles were selected in stress-controlled tests (since the developed shear strain changes with the increase in loading cycles). It can be observed that the evaluated shear modulus obtained from both strain-controlled and stress-controlled approach follow similar degradation pattern with minimal difference from each other (Fig. 14a). Figure 14b reflects the variations of damping ratio obtained from stress-controlled and strain-controlled approaches. It can be noted that the damping ratio attains the peak magnitude at $\gamma \approx 1\%$ from both the approaches. Beyond the peak values of 1% shear strain, a significant reduction in damping ratio is observed at higher strain levels, which is

appreciable disagreement to the results obtained from previous experimental studies (Seed and Idriss 1970; Iwasaki et al. 1978; Kokusho 1980; Seed et al. 1986; Vucetic and Dobry 1991; Stokoe et al. 1995; Govindaraju 2005; Kirar and Maheshwari 2013). Earlier studies reported the damping ratio up to strain levels of about 1% obtained through strain-controlled approach. Very few literatures are available on the application of strain-controlled approach to experimentally estimate the damping ratio beyond 1% shear strain, which followed a similar trend as obtained in the present study (Kiku and Yoshida 2000; Brennan et al. 2005; Mashiri 2014; Matasovic and Vucetic 1993). The damping ratio obtained from strain and stress-controlled approach follow similar trend, and

hence, it can be concluded that the dynamic soil properties can be evaluated by both the approaches. However, due to asymmetry in hysteresis loop and shear strains after a few loading cycles, the stress-controlled approach mislead the accuracy of dynamic properties. In such condition, strain-controlled approach would be more suitable option to evaluate the accurate dynamic properties for any constant shear strain amplitudes.

7 Conclusions

This study investigated the response of cohesionless BS soil subjected to the strain-controlled and stress-controlled cyclic triaxial tests. Based on the present study, the following conclusions were drawn:

1. During strain-controlled cyclic loading, the developed excess PWP ratio is strongly influenced by the applied cyclic shear strain amplitude. For higher magnitudes of the latter, smaller number of loading cycles are required to attain the state of liquefaction.
2. The strain-controlled tests dictate that the excess PWP ratio nearly attains the magnitude of 1 when the shear strain amplitude approximately reaches 0.75% and the corresponding CSR becomes approximately equal to 0.5. Beyond this strain level, BS soil manifests the onset of liquefaction right at the 1st loading cycle, and thus, CSR = 0.5 can be considered as the limiting condition to attain liquefaction in BS specimens subjected to strain-controlled loading.
3. Based on the strain-controlled tests, the liquefaction potential of a soil specimen decreases with increasing confining pressure and relative density, owing to the smaller development of excess PWP in successive loading cycles, thus requiring higher number of loading cycles to initiate liquefaction of the BS specimens. On the contrary, in a stress-controlled test, an increase in CSR leads to higher magnitudes of applied deviatoric stress and correspondingly higher excess PWP. Hence, the number of cycles required to achieve the onset of liquefaction decreases with the increase in the confining pressure. Similar behaviour is manifested for samples prepared at higher relative densities. As a consequence, loose saturated BS specimens are susceptible to liquefaction even at low shaking, while the denser samples are comparatively resilient during a stress-controlled loading.
4. Based on stress-controlled investigations of BS soil, $\gamma = 0.5\%$ is recommended as the limiting value beyond which the onset of liquefaction is prominent in BS samples prepared at various relative densities and subjected to varying confining pressures.
5. For progressive loading cycles, the excess PWP generated in a stress-controlled test is considerably larger than that generated in a strain-controlled approach. Hence, estimation of dynamic properties would depend significantly on the testing methodology if higher load cycles are used, as considered conventionally. The generation of excess PWP being nearly similar in the first loading cycle of either stress- or strain-controlled approaches, it is recommended to estimate the dynamic soil properties using the 1st loading cycle from the tests.
6. The estimation of dynamic properties from strain controlled tests are recommended to be preferred owing to the equal magnitudes of strain generated in the compression and extension phases, which is not the case for stress-controlled hysteresis wherein the strain in the compression phase largely supersedes that generated in the extension phase.
7. In contrary to the strain-controlled approach, since the stress-controlled approach result in the simultaneous accumulation of excess PWP and shear strains which is a more realistic representation of field condition during a seismic activity, the same is recommended for the evaluation of liquefaction potential of soil specimens.

References

- ASTM D0854 (2014) Standard test methods for specific gravity of soil solids by water pycnometer. ASTM International, West Conshohocken. <https://doi.org/10.1520/D0854-14>
- ASTM D2487 (2011) Standard practice for classification of soils for engineering purposes (Unified Soil Classification System). ASTM International, West Conshohocken. <https://doi.org/10.1520/D2487-11>

- ASTM D3999/D3999 M (2011) Standard test methods for the determination of the modulus and damping properties of soils using the cyclic triaxial apparatus. ASTM International, West Conshohocken. https://doi.org/10.1520/D3999_D3999M
- ASTM D4253-16 (2016) Standard test methods for maximum index density and unit weight of soils using a vibratory table. ASTM International, West Conshohocken. <https://doi.org/10.1520/D4253-16>
- ASTM D4254-16 (2016) Standard test methods for minimum index density and unit weight of soils and calculation of relative density. ASTM International, West Conshohocken. <https://doi.org/10.1520/D4254-16>
- ASTM D5311 (2011) Test method for load controlled cyclic triaxial strength of soil. Annual book of ASTM standards. ASTM International, West Conshohocken
- ASTM D6913/D6913 M (2017) Standard test methods for particle-size distribution (gradation) of soils using sieve analysis. ASTM International, West Conshohocken. https://doi.org/10.1520/D6913_D6913M-17
- Bhattacharya S (2007) Design and foundations in seismic areas: principles and applications. National information Centre of Earthquake Engineering, IIT Kanpur, India, pp. 477
- Brennan AJ, Thusyanthan NI, Madabhushi SPG (2005) Evaluation of shear modulus and damping in dynamic centrifuge tests. *J Geotech Geoenviron Eng* 131:1488–1497
- Byrne PM, Park SS, Beaty M, Sharp M, Gonzalez L, Abdoun T (2004) Numerical modeling of liquefaction and comparison with centrifuge tests. *Can Geotech J* 41:193–211
- Castro G (1975) Liquefaction and cyclic mobility of saturated sand. *J Geotech Eng ASCE* 113(8):827–845
- Chattaraj R, Sengupta A (2016) Liquefaction potential and strain dependent dynamic properties of Kasai river sand. *Soil Dyn Earthq Eng* 90:467–475
- Chattaraj R, Sengupta A (2017) Liquefaction potential and strain dependent dynamic properties of Kasai River sand. *Soil Dyn Earthq Eng* 90:467–475
- Dammala PK, Kumar SS, Krishna AM, Bhattacharya S (2019) Dynamic soil properties and liquefaction potential of northeast Indian soil for non-linear effective stress analysis. *Bull Earthq Eng* 17(6):2899–2933
- Dobry R, Ladd RS, Yokel FY, Chung RM, Powell D (1982) Prediction of pore water pressure buildup and liquefaction of sand during earthquakes by the cyclic strain method. National Bureau of Standards Building Science Series 138, Washington, p 154
- Elgamal AW, Zeghal M, Taboada V, Dobry R (1996) Analysis of site liquefaction and lateral spreading using centrifuge testing records. *Soils Found* 36:111–121
- Govindaraju L (2005) PhD thesis, Indian Institute of Science, Bangalore
- Ishihara K (1993) Liquefaction and flow failure during earthquakes. *Geotechnique* 43(3):351–451
- Ishihara K (1996) Soil behaviour in earthquake geotechnics. Oxford Science Publications, Oxford
- Ishihara K, Yasuda S (1972) Soil liquefaction due to irregular excitation. *Soils Found* 12:65–77
- Ishihara K, Troncoso J, Kawase Y, Takahashi Y (1980) Cyclic strength characteristics of tailings materials. *Soils Found* 20(4):127–142
- Iwasaki T, Tatsuoka F, Takagi Y (1978) Shear modulus of sands under torsional shear loading. *Soils Found* 18(1):39–56
- Jakka RS, Datta M, Ramana GV (2010) Liquefaction behaviour of loose and compacted pond ash. *Soil Dyn Earthq Eng* 30:580–590
- Kiku H, Yoshida N (2000) Dynamic deformation property tests at large strains. In Proceedings of 12th world conference on earthquake engineering, New Zealand
- Kirar B, Maheshwari BK (2013) Effects of silt content on dynamic properties of solani sand. In: 7th international conferences on case histories in geotechnical engineering, Chicago
- Kokusho T (1980) Cyclic triaxial test of dynamic soil properties for wide strain range. *Soils Found* 20(2):45–60
- Kramer SL (1996) Geotechnical earthquake engineering. Prentice Hall, New Jersey
- Kumar SS, Dey A, Krishna AM (2015) Cyclic response of sand using stress-controlled cyclic triaxial tests. In: Proceedings of Indian geotechnical conference, 2015, Pune, India, Paper No. 242
- Kumar SS, Krishna AM, Dey A (2017a) Evaluation of dynamic properties of sandy soil at high cyclic strains. *Soil Dyn Earthq Eng* 99:157–167
- Kumar SS, Krishna AM, Dey A (2017b) High strain dynamic properties of perfectly dry and saturated cohesionless soil. *Indian Geotech J* 48(3):549–557
- Kumar SS, Dey A, Krishna AM (2018a) Importance of site-specific dynamic soil properties for seismic ground response studies. *Int J Geotech Earthq Eng* 9(1):78–98
- Kumar SS, Dey A, Krishna AM (2018b) Response of saturated cohesionless soil subjected to irregular seismic excitations. *Nat Hazards* 93(1):509–529
- Ladd RS, Dobry R, Dutko P, Yokel FY, Chung RM (1989) Pore-water pressure build-up in clean sands because of cyclic straining. *Geotech Test J* 12(1):77–86
- Lee KL, Seed HB (1967) Cyclic stress conditions causing liquefaction of sand. *J Soil Mech Found Eng ASCE* 93(1):47–70
- Lombardi D, Bhattacharya S, Hyodo M, Kaneko T (2014) Undrained behaviour of two silica sands and practical implications for modelling SSI in liquefiable soils. *Soil Dyn Earthq Eng* 66:293–304
- Maheshwari BK, Kale SS, Kaynia AM (2012) Dynamic properties of Solani sand at large strains: a parametric study. *Int J Geotech Eng* 6:353–358
- Mashiri MS (2014) Monotonic and cyclic behaviour of sand-tire chip (STCh) mixtures. Dissertation School of Civil, Mining and Environmental Engineering, University of Wollongong, p 290
- Matasovic N, Vucetic M (1992) A pore pressure model for cyclic straining of clay. *Soils Found* 32(3):156–173
- Matasovic N, Vucetic M (1993) Cyclic characterization of liquefiable sands. *J Geotech Geoenviron Eng* 119(11):1805–1822
- Movahed V, Sharafi H, Baziar M, Shahnazari H (2011) Comparison of strain controlled and stress controlled tests in evaluation of fines content effect on liquefaction of sands—an energy approach. In: Han J, Alzamora DE (eds) *Geo-Frontiers*. ASCE, Dallas, pp 1804–1814
- Peck RB (1979) Liquefaction potential: science versus practice. *J Geotech Eng ASCE* 105(5):553–562

- Poddar SMC (1950) A short note on the Assam earthquake of August 15, 1950. A compilation of papers on the Assam earthquake of August 15, 1950, Government of India 1953
- Qu M, Xie Q, Cao X, Zhao W, He J, Jin J (2016) Model test of stone columns as liquefaction countermeasure in sandy soils. *Front Struct Civ Eng* 10:481–487
- Raghukanth STG (2008) Simulation of strong ground motion during the 1950 great Assam earthquake. *Pure appl Geophys* 165:1761–1787
- Ravishankar BV, Sitharam TG, Govindaraju L (2005) Dynamic properties of Ahmedabad sands at large strains. In: *Pro Indian geotechnical conference, Ahmedabad, India*, pp 369–372
- Seed HB (1968) Design problems in soil liquefaction. *J Geotech Eng ASCE* 113(8):827–845
- Seed HB, Idriss IM (1970) Soil moduli and damping factors for dynamic response analyses. Report EERC 70-10. Earthquake Engineering Research Centre, University of California, Berkeley
- Seed HB, Lee KL (1966) Liquefaction of saturated sands during cyclic loading. *J Soil Mech Found ASCE* 92(6):105–134
- Seed HB, Peacock WH (1971) Test procedures for measuring soil liquefaction characteristics. *J Soil Mech Found ASCE* 101(6):551–569
- Seed HB, Wong RT, Idriss IM, Tokimatsu K (1986) Moduli and damping factors for dynamic analysis of cohesionless soils. *J Geotech Eng* 112(11):1016–1032
- Simatupang M, Okamura M (2017) Liquefaction resistance of sand remediated with carbonate precipitation at different degrees of saturation during curing. *Soils Found* 57(4):619–631
- Sitharam TG, Ravishankar BV, Patil SM (2012) Liquefaction and pore water pressure generation in sand: cyclic strain controlled triaxial tests. *Int J Geotech Earthq Eng* 3(1):57–85
- Sreng S, Okochi Y, Kobayashi K, Tanaka H, Sugiyama H, Kusala T, Miki H, Makino M (2015) Centrifuge model tests of embankment with a new liquefaction countermeasure by ground improvement considering constraint effect. In: *6th international conference on earthquake geotechnical engineering*, 1–4 November 2015, Christchurch, New Zealand
- Stokoe KH, Hwang SH, Lee JNK, Andrus RD (1995) Effects of various parameters on the stiffness and damping of soils at small to medium strains. In: *Proceedings of the first international conference on pre-failure deformation characteristics of geomaterials, Sapporo, Japan, Pre-failure deformation of geo-materials*. A. A. Balkema, pp 785–816
- Teachavorasinskun S, Thongchim P, Lukkunaprasit P (2002) Shear modulus and damping of soft Bangkok clays. *Can Geotech J* 39:1201–1208
- Tumi HOZ (1983) Effect of confining pressure and particle angularity on resistance to liquefaction. M. Sc. Thesis, University of British Columbia. <https://doi.org/10.14288/1.0062968>
- Vucetic M, Dobry R (1988) Cyclic triaxial strain-controlled testing of liquefiable sands. In: Donaghe RT, Chaney RC, Silver ML (eds) *Advanced triaxial testing soil and rock*. ASTM, West Conshohocken, p 475
- Vucetic M, Dobry R (1991) Effect of soil plasticity on cyclic response. *J Geotech Eng ASCE* 117(1):89–107
- Xenaki VC, Athanasopoulos GA (2003) Liquefaction resistance of sand-mixtures: an experimental investigation of the effect of fines. *Soil Dyn Earthq Eng* 23:183–194
- Yilmaz MT, Pekcan O, Bakir BS (2004) Undrained cyclic shear and deformation behaviour of silt-clay mixtures of Adapazari, Turkey. *Soil Dyn Earthq Eng* 24:497–507
- Youd TL, Idriss IM, Andrus RD, Arango I, Castro G, Christian JT, Dobry R, Finn WDL, Harder LF Jr, Hynes ME, Ishihara K, Koester JP, Liao SSC, Marcuson WF III, Martin GR, Mitchell JK, Moriwaki Y, Power MS, Robertson PK, Seed RB, Stokoe KH II (2001) Liquefaction resistance of soils: summary report from the 1996 NCEER and 1998 NCEER/NSF workshops on evaluation of liquefaction resistance of soils. *J Geotech Geoenviron Eng* 127:817–833

Publisher's Note Springer Nature remains neutral with regard to jurisdictional claims in published maps and institutional affiliations.